

## Determination of the hydrogen diffusion mechanism in $\gamma$ -titanium hydride using nuclear magnetic resonance

L. D. Bustard\* and R. M. Cotts

*Laboratory of Atomic and Solid State Physics, Cornell University, Ithaca, New York 14853*

E. F. W. Seymour

*Department of Physics, University of Warwick, Coventry CV4 7AL, United Kingdom*

(Received 29 March 1979)

In the  $\gamma$  phase of  $\text{TiH}_x$ , hydrogen atoms are known to occupy the tetrahedral interstitial sites which form a simple cubic sublattice in the fcc titanium host. To determine to which nearest-neighbor site diffusing H atoms jump during their migration through the lattice, NMR measurements of (i) the hydrogen diffusion coefficient  $D$ , between 450 and 550 °C and (ii) the proton-spin-system longitudinal relaxation time,  $T_1$ , between 80 and 550 °C are presented for  $\text{TiH}_{1.55}$  and  $\text{TiH}_{1.71}$ . From the relationship  $D = f_T L^2 / (6\tau_d)$ , the jump length  $L$  is determined from the measured  $D$  values and values of the mean residence time between atomic hops  $\tau_d$ , calculated from  $T_1$  data. The tracer correlation factor  $f_T$  is obtained from the literature. The diffusion and  $T_1$  relaxation data are shown to be consistent with a first-nearest-neighbor hopping model.

### I. INTRODUCTION

In the  $\gamma$  phase of the titanium-hydrogen system it is known that the hydrogen ions occupy the tetrahedral interstitial sites of the fcc structured titanium,<sup>1,2</sup> there being two such sites for each metal atom. These sites form a simple cubic lattice. An experimental determination of the elementary jump step has not previously been reported. Nuclear magnetic resonance of the protons presents a method for determining the elementary jump step. The pulsed-magnetic-field-gradient technique can measure the self-diffusion coefficient,  $D$ , for hydrogen motion. From measurements of the spin-lattice relaxation time  $T_1$  the mean residence time between atomic hops  $\tau_d$ , can be determined. These two quantities are related to the jump length  $L$ , and the tracer correlation factor  $f_T$ , by

$$D = f_T \frac{L^2}{6\tau_d} \quad (1)$$

Hence, ideally at least, the jump length may be calculated if diffusion and spin-lattice relaxation measurements are performed. Until recently, this method of determining  $L$  has not been widely employed because of the inaccuracy of many of the theoretical models for relating  $\tau_d$  to  $T_1$ . Good tabulated calculations now exist for the extreme limits of very low<sup>3</sup> (monovacancy) and very high<sup>3,4</sup> (random-walk) vacancy concentrations. Here, vacancy means a vacant tetrahedral interstitial site. A new method of calculation, described by Fedders and Sankey,<sup>5</sup> applies to intermediate vacancy calculations. In the preceding paper, Bustard<sup>6</sup> discusses this problem and uses an

independent-spin-pair (ISP) calculation to relate  $\tau_d$  and  $T_{1d}$ , where  $(T_{1d})^{-1}$  is the NMR relaxation rate due to diffusion only. He performs his calculations via Monte Carlo techniques for the cases of first-nearest-neighbors (1NN) and third-nearest-neighbor (3NN) hopping on a simple cubic lattice. He shows that on the the high-temperature side of the  $T_1$  minimum his computer simulations have a random uncertainty of  $\pm 3\%$  and a systematic uncertainty less than 6%.

With Bustard's calculations, Eq. (1) can be used to determine the jump length for hydrogen hopping in  $\gamma$ - $\text{TiH}_x$ , with vacancy concentration of  $\frac{1}{2}(2-x)$ . We report on both  $T_1$  and  $D$  measurements performed on  $\text{TiH}_{1.55}$  and  $\text{TiH}_{1.71}$  hydride samples. These concentrations were chosen as having significantly different vacancy concentrations and for also allowing comparison with previous measurements.

An outline of the remaining sections of this paper is: Sec. II presents a historical survey of studies performed on the  $\gamma$ - $\text{TiH}_x$  system. Section III details our sample preparation techniques. Section IV discusses the diffusion measurements and Sec. V the  $T_1$  measurements. Section VI analyzes the diffusion and  $T_1$  relaxation data to obtain the jump length and Sec. VII presents a summary of the results.

### II. HISTORICAL SURVEY

The  $\gamma$  phase of  $\text{TiH}_x$  ( $1.5 \leq x \leq 2.0$ ) was shown by Sidhu, Heaton, and Zaubers<sup>1</sup> to have a face-centered-cubic arrangement of titanium atoms. Stalinski, Coogan, and Gutowsky<sup>2</sup> used NMR

second-moment analysis to establish that the hydrogen nuclei randomly occupy the tetrahedral positions within the fcc titanium structure. These positions form a simple cubic lattice. Stalinski *et al.* also determined that the diffusion rate is directly proportional to the number of vacancies in the hydrogen lattice. This indicates that hydrogen motion takes place via a vacancy mechanism. Coogan and Gutowsky<sup>7</sup> suggested that the hydrogen jump path is along the hydrogen cube diagonal through the vacant octahedral site. This corresponds to the hydrogen atom jumping from one tetrahedral interstitial position to a third-nearest-neighbor position.

Korn and Zamir<sup>8</sup> have made an extensive set of  $T_1$  measurements from 25 to 500 °C for several different hydrogen concentrations in the  $\gamma$  phase of  $\text{TiH}_x$ . They confirm the proportionality of  $D$  with vacancy concentration and they measure an activation energy  $E_A$  for hydrogen motion of 0.51 eV which is independent of hydrogen concentration. Stalinski *et al.* observed a small dependence of activation energy upon concentration. Schmolz and Noack<sup>9</sup> agree with Korn and Zamir that the activation energy is independent of vacancy concentration and obtain  $E_A = 0.50$  eV. Weaver and VanDyke<sup>10</sup> confirm that for  $\gamma\text{-TiH}_{1.55}$  the hydrogen is located at the tetrahedral interstitial positions. Bisson and Wilson<sup>11</sup> perform theoretical calculations of hydrogen motion in  $\gamma\text{-TiH}_x$  and conclude

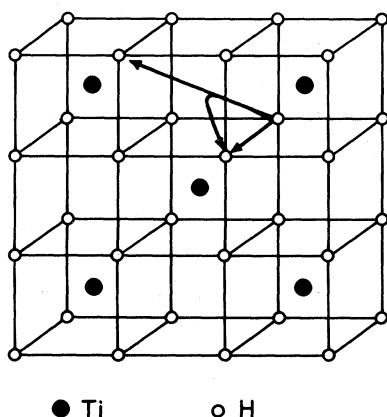


FIG. 1.  $\gamma\text{-TiH}_x$  phase has the  $\text{CaF}_2$  structure. The titanium atoms form a fcc structure with a lattice constant (Ref. 19) equal to 4.44 Å. The hydrogen randomly occupies the tetrahedral interstitial positions which form a simple cubic lattice. Theoretical calculations of Bisson and Wilson (Ref. 11) indicate that the two most likely diffusion jump paths for hydrogen are from a tetrahedral position through the octahedral site to nearest- and third-nearest-neighbor tetrahedral sites. The octahedral sites lie at those body centers of the simple cubic hydrogen lattice not occupied by Ti atoms. Titanium atoms situated in half the simple cube centers prevent jumps to half of the third-nearest-neighbor sites, but octahedral sites are available for indirect paths to all first neighbor sites.

that the diffusion mechanism yielding the lowest migration energy is hydrogen motion to a first-nearest-neighbor position via a "curved" path through the octahedral site. For this jump  $E_A$  is predicted to be 0.58 eV. For motion through the octahedral site to second- and third-nearest neighbors, they calculate activation energies of 0.69 and 0.65 eV, respectively. By contrast, the energy barriers for hydrogen motion along the  $\langle 100 \rangle$  and  $\langle 110 \rangle$  directions are 1.2 and 2.3 eV, respectively.

Figure 1 summarizes the structure of  $\gamma\text{-TiH}_x$ . The predicted predominant jumps to first- and third-nearest neighbors are also shown. Note that Eq. (1) cannot be used to distinguish between straight line and curved paths for any jump mechanism. It can only determine the distance between end points of the motion.

### III. SAMPLE PREPARATION

Marz grade titanium rods obtained from the Materials Research Corporation<sup>12</sup> were used to make the hydride samples. The rods were washed in a mild  $\text{HF-HNO}_3$  solution and then outgassed to pressures less than  $10^{-5}$  Torr. The titanium was heated to 600 °C and then gradually cooled to room temperature in the presence of hydrogen gas. This process was repeated twice. The first time produced a brittle hydride which was ground with mortar and pestle to 149–210  $\mu\text{m}$  sizes. These particles were then weighed and outgassed. A second hydriding produced the desired hydrogen concentration, which was determined by pressure, volume, and temperature measurements of the hydrogen gas over the sample. This procedure yielded  $\text{TiH}_x$  samples accurate in  $x$  to  $\pm 0.03$ .

To improve the accuracy of the diffusion measurements (see Sec. IV) and to prevent sintering of the hydride at the 500 °C temperatures required to measure the diffusion coefficient, ground quartz glass particles were mixed in a one-to-one ratio with the titanium hydride. The resulting samples were sealed in quartz vials.

Several polycrystals from the  $\text{TiH}_{1.55}$  and  $\text{TiH}_{1.71}$  samples were examined using the scanning electron microscope of the Cornell Materials Science Center. This examination confirmed that cracks in the polycrystals would not cause bounded diffusion effects<sup>13</sup> during the pulsed-magnetic-field-gradient diffusion measurements.

### IV. DIFFUSION MEASUREMENTS

The diffusion coefficient was measured by the stimulated echo pulsed-magnetic-field-gradient techniques of Tanner.<sup>14</sup> Figure 2 illustrates this technique. The attenuation of the echo signal,  $S$ , is given

by

$$S(\tau_1 + \tau_2) = \frac{1}{2} S_0 \exp \left\{ \frac{\tau_1 - \tau_2}{T_1} - \frac{2\tau_1}{T_2} - \gamma^2 D \left[ \tau_1^2 \left( \tau_2 - \frac{1}{3} \tau_1 \right) G_0^2 + \left( \Delta - \frac{1}{3} \delta \right) \delta^2 G^2 - [t_1^2 + t_2^2 + \delta(t_1 + \delta_2) + \frac{2}{3} \delta^2 - 2\tau_1 \tau_2] \delta \vec{G} \cdot \vec{G}_0 \right] \right\}, \quad (2)$$

where  $G_0$  is any time-independent background field gradient which happens to be present. With the stimulated-echo technique, diffusion measurements were possible even though the spin-spin relaxation times  $T_2$ , were too short for a  $90^\circ$ - $\tau$ - $180^\circ$  pulsed-magnetic-field-gradient technique to accurately measure the diffusion coefficient. Because of some background gradient effects,  $T_2$  was substantially shorter than  $T_1$  for many  $\gamma$ -TiH<sub>x</sub> samples. In the stimulated echo technique,  $T_1$  and not  $T_2$  limits one's ability to measure  $D$ .

The diffusion coefficients of TiH<sub>1.55</sub> and TiH<sub>1.71</sub> samples near 450°C are of the order  $10^{-7}$  cm<sup>2</sup>/sec. This is close to the lower limit of the capability of the pulsed-gradient technique. Measurements of  $D$  for lower temperatures were not practicable. The partial pressure of hydrogen rapidly increases for temperatures above 550°C. Since this effect introduces the danger of fracture of the quartz vial, measurements of  $D$  were not taken for temperatures above ~550°C. Diffusion measurements are therefore limited to the temperature range of about 450 to 550°C.

The presence of background gradients<sup>13</sup> can have a

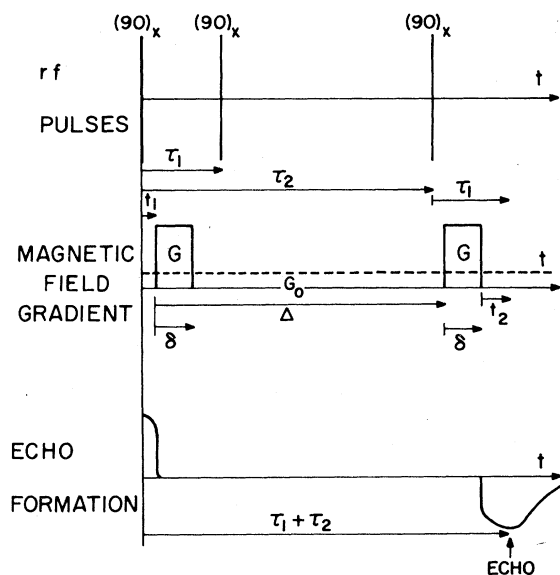


FIG. 2. Stimulated-echo method of measuring diffusion coefficients.

severe effect on the accuracy of diffusion measurements performed on  $\gamma$ -TiH<sub>x</sub>. The echo attenuation for the stimulated echo sequence does have a  $\vec{G} \cdot \vec{G}_0$  [see Eq. (2)] dependence. Murday and Cotts<sup>13</sup> have applied a series expansion of the  $\vec{G} \cdot \vec{G}_0$  term for the analysis of the Stejskal and Tanner<sup>15</sup> pulsed-gradient technique. A similar analysis performed for the stimulated-echo technique yields the following approximate inequality for the diffusion coefficient:

$$D_{\text{measured}} < D < D_{\text{measured}} + \frac{1}{2} \gamma^2 D_{\text{measured}}^2 \tau_*^4 \langle G_0^2 \rangle / (\Delta - \frac{1}{3} \delta) .$$

Here

$$\tau_*^2 = [t_1^2 + t_2^2 + \delta(t_1 + t_2) + \frac{2}{3} \delta^2 - 2\tau_1 \tau_2] . \quad (3)$$

and for the measurements performed at constant  $\tau_1$  and  $\tau_2$

$$\langle G_0^2 \rangle = \int_{-G_1}^{G_1} \rho(G_0) G_0^2 dG_0 . \quad (4)$$

Use of Eq. (3) requires an evaluation of  $\langle G_0^2 \rangle$  which in turn necessitates the determination of  $\rho(G_0)$ , the  $G_0$  distribution function. In practice and theory this is not possible.

A rough estimate of  $\langle G_0^2 \rangle$  can be obtained from consideration of Eq. (2). First  $T_1$  is measured by standard methods. Second, an approximate value of  $D$  is obtained from application of Eq. (2) to a pulsed-gradient experiment in which  $\langle G_0^2 \rangle$  is assumed to be negligible. The echo height  $S(\tau_1 + \tau_2)$  is then measured for various values of  $\tau_2$  with  $\tau_1$  held constant and  $\vec{G} = 0$ . From Eq. (2)

$$\ln [2S(\tau_1 + \tau_2)/S_0] = \frac{(\tau_1 - \tau_2)}{T_1} - \frac{2\tau_1}{T_2} - \gamma^2 D \tau_1^2 \left( \tau_2 - \frac{1}{3} \tau_1 \right) G_0^2 , \quad (5)$$

and the above values of  $T_1$  and  $D$ ,  $G_0^2$  is found and used as our estimate of  $\langle G_0^2 \rangle$ . The value of  $\langle G_0^2 \rangle$  so obtained represents the effects of the distribution of background gradients upon the stimulated echo. From the inequality above, an estimation can be made of the error in  $D$  caused by  $\langle G_0^2 \rangle$ .

For some of our initial samples the uncertainty in  $D$  was as large as a factor of 2. By mixing ground quartz with the hydride particles, the uncertainty was substantially reduced. Large particle size (149 to 210  $\mu$ m) and a low resonance frequency (7 MHz) also

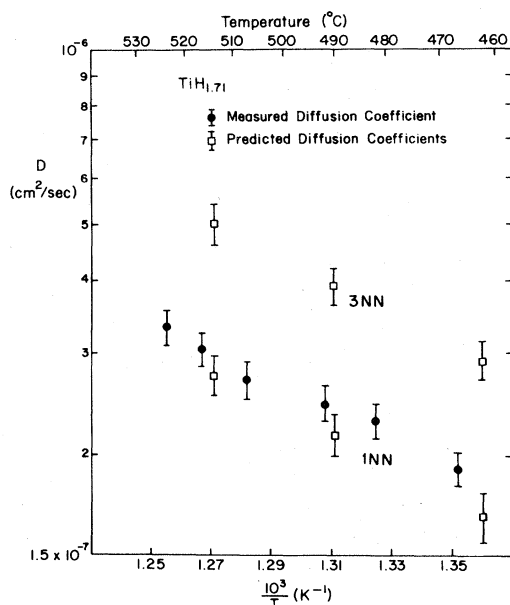


FIG. 3. Measured and predicted values of the diffusion coefficients for  $\text{TiH}_{1.71}$ . Predicted values are based on calculations by the first method discussed in Sec. VI.

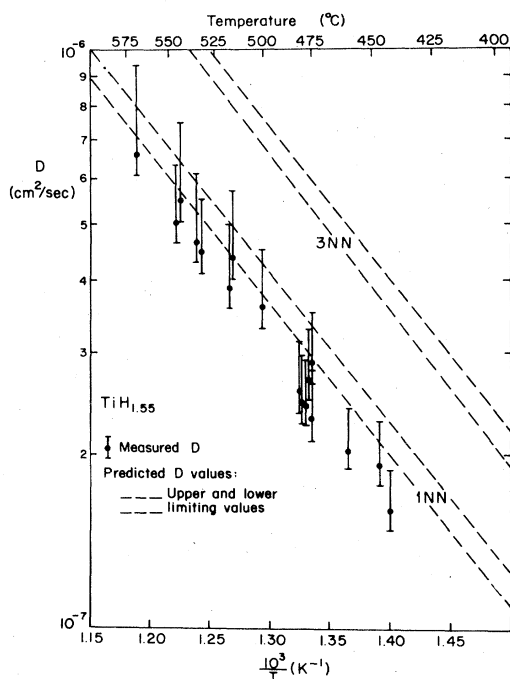


FIG. 4. Measured and predicted values of the diffusion coefficients for  $\text{TiH}_{1.55}$ . Predicted values are based on calculations by the first method discussed in Sec. VI and correspond to the straight line in Fig. 7.

helped minimize background gradients. Uncertainties computed from Eq. (3) as well as a  $\pm 8\%$  error caused by time interval and applied gradient measurements are included in the error bars of  $D$  plotted in Figs. 3 and 4, which present the measured diffusion coefficients for  $\text{TiH}_{1.71}$  and  $\text{TiH}_{1.55}$ , respectively.

To use Eq. (1) and the measured diffusion coefficient to calculate the jump length, the tracer correlation factor must be known. DeBruin and Murch,<sup>16</sup> using computer simulation techniques, show for first-nearest-neighbor hopping of noninteracting atoms on a simple cubic lattice that  $f_T = 0.71$  for 15% vacancy concentration and  $f_T = 0.75$  for 22.5% vacancy concentration.

Third-nearest-neighbor hopping in  $\gamma\text{-TiH}_x$  corresponds to hopping on a diamond structure lattice. For monovacancies it is well known that  $f_T = 0.50$ . Calculations for 15% and 22.5% vacancy concentrations have not been performed. Murch<sup>17</sup> indicates that to first approximation  $f_T$  may be considered to vary linearly between its two limiting values for monovacancies and random walk. This yields  $f_T = 0.58$  for 15% vacancy concentration and  $f_T = 0.61$  for 22.5% vacancy concentration.

## V. SPIN-LATTICE RELAXATION MEASUREMENTS

$T_1$  data for the  $\text{TiH}_{1.71}$  and  $\text{TiH}_{1.55}$  samples are presented in Figs. 5 and 6, respectively. For both concentrations the results of Korn and Zamir<sup>8</sup> are given for comparison purposes. Note that our  $\text{TiH}_{1.71}$  data (Fig. 5) show some scatter on the high-temperature side near to the  $T_1$  minimum. Korn and Zamir also observed small glitches for some of their  $T_1$  curves. Recently, Fedders and Sankey<sup>5</sup> have predicted the occurrence of such a glitch for the hopping model of 1NN jumps on a 15% vacant simple cubic (sc) lattice.

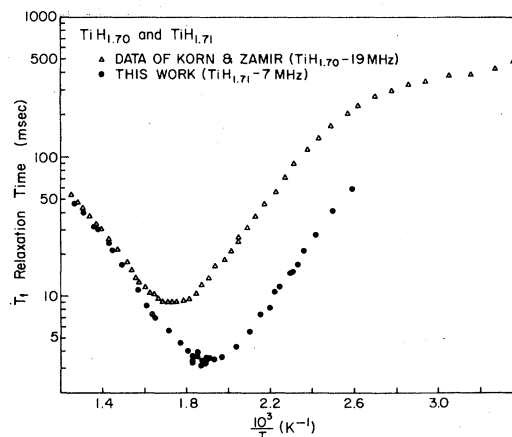


FIG. 5.  $T_1$  relaxation data for  $\text{TiH}_{1.70}$  and  $\text{TiH}_{1.71}$  hydrides.

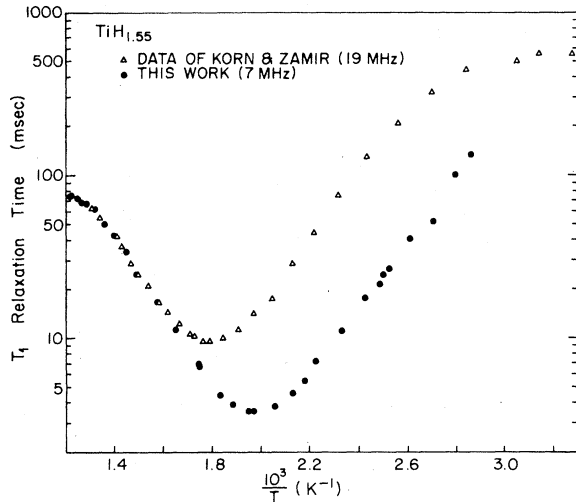


FIG. 6.  $T_1$  relaxation data for  $\text{TiH}_{1.55}$ .

The value of  $T_{1d}$  is obtained from the measured  $T_1$  from

$$\frac{1}{T_1} = \frac{1}{T_{1d}} + \frac{1}{T_{1e}} \quad (6)$$

It is commonly found that the conduction-electron contribution  $(T_{1e})^{-1}$  is proportional to the absolute temperature  $T$ , and we assume that this relationship holds for this case also. We define  $K = T_{1e}T$ , where  $K$  (frequently referred to as the Korringa constant) has been extensively studied as a function of vacancy concentration in  $\gamma$ -titanium hydride (Fig. 9 in Ref. 9). The values of  $K$  determined by Korn and Zamir from a range where  $T_{1d}$  was of minor importance are in reasonable agreement to those reported by other workers, and they predict that  $K = 190 \text{ sec K}$  for  $\text{TiH}_{1.55}$  and  $K = 124 \text{ sec K}$  for  $\text{TiH}_{1.71}$ .

## VI. DETERMINATION OF THE ELEMENTARY DIFFUSION STEP LENGTH

To elucidate information concerning the diffusion jump mechanism,  $\tau_d$  must be calculated using  $T_1$  relaxation information. This involves the use of  $T_1$  relaxation models which include the jump mechanism as an assumption of the model. We considered the two models of 1NN and 3NN hopping presented in the previous paper by Bustard.<sup>6</sup> Both models are single activation energy models. The possibility that hydrogen spins may jump via both 1NN and 3NN hops described by different activation energies is not considered. The omission of this refinement is due to the theoretical difficulties encountered in generating an accurate  $T_1$  relaxation model to describe a situation with a mixture of jump mechanisms. As the

temperature is varied, the ratio of spins performing one type of jump to those performing a second type of jump would vary if the activation energies describing those jump paths differ.

There is some choice in procedure in analyzing our  $T_1$  data and we present 2. The first has the merit that it makes no assumptions concerning the temperature dependence of diffusion over the range of  $T_1$  and  $D$  data, but it does require knowledge of  $T_{1e}$ . For this case, values of  $K$  from the literature as cited in Sec. V are used. The second method assumes that the temperature dependence of  $\tau_d$  is described by a single activation energy and that the Korringa relationship holds.  $T_1$  data for each sample can then be fitted to Bustard's calculation relating  $T_{1d}$  to  $\tau_d$  with  $K$ , the activation energy, and preexponential factor as fitting parameters.

In the first method, for both 1NN and 3NN jump mechanisms, Bustard's<sup>6</sup> high-temperature calculations of  $T_{1d}$  vs  $\omega\tau_d$  were used to calculate  $\tau_d$  as a function of temperature. This was done by forming the experimental ratio of  $(T_{1d}/T_{1d_{\min}})$  and comparing it to calculated theoretical values.  $T_{1d}$  data were calculated from  $T_1$  measurements using the predicted Korringa constants given in Sec. V. Since it has recently been shown<sup>5</sup> that the value of  $T_{1d}$  at the minimum is almost independent of the jump mechanism, this method of calculating  $\tau_d$  does not require any assumptions regarding possible variations in activation energy between the temperatures at which  $T_{1d_{\min}}$  and the particular  $T_{1d}$  are measured. The only interaction to be considered is that between protons; the contribution of titanium nuclei to the proton  $T_1$  is very small.

As well as depending on the accuracy of the original  $T_1$  measurements and the assumed model computations of  $T_{1d}$  vs  $\omega\tau_d$ , the accuracy of this technique of calculating  $\tau_d$  relies on (i) the assumption that the value of  $T_{1d_{\min}}$  is independent of variations in jump model, and (ii) the use of predicted Korringa constants based on Korn and Zamir's data.

Table I is representative of the variation in the literature for  $(\alpha T_1)_{\max}^{-1}$  values for hopping on a sc lattice. The value of  $\alpha$

$$\alpha = \frac{c\hbar^2\gamma^4 I(I+1)}{5\omega b^6} \quad (7)$$

allows  $T_1^{-1}$  values to be listed without specifying the spin-spin separation  $b$ , nor the frequency  $\omega$ . The spin concentration is  $c$ . The maximum variation for  $(\alpha T_1)_{\max}^{-1}$  in Table I is 13%. The variation between Bustard's 15% vacancy concentration 1NN and 3NN hopping models, is less than 1%.

Clearly, since our sample concentrations may disagree somewhat from those used by Korn and Zamir, the use of Korringa constants predicted from their data does introduce some possible error into our

TABLE I. Values of  $(\alpha T_1)_{\max}^{-1}$  for different  $T_1$  relaxation models describing spin diffusion on a simple cubic lattice,  $\alpha = c\hbar^2\gamma^4 I(I+1)/5\omega b^6$ .

$T_1$ relaxation model	$(\alpha T_1)_{\max}^{-1}$
1NN random walk (Barton and Sholl <sup>a</sup> )	21.72
3NN random walk (Barton and Sholl <sup>b</sup> )	21.78
1NN random walk (Wolf <sup>c</sup> )	21.62
1NN monovacancies (Wolf <sup>c</sup> )	20.74
1NN 15% vacancy concentration (Fedders and Sankey <sup>d</sup> )	21.7
1NN $3.75 \times 10^{-5}$ vacancy concentration (Bustard <sup>e</sup> )	22.3
1NN 15% vacancy concentration (Bustard <sup>e</sup> )	19.7
1NN 90% vacancy concentration (Bustard <sup>e</sup> )	21.7
3NN 15% vacancy concentration (Bustard <sup>e</sup> )	19.6
3NN 90% vacancy concentration (Bustard <sup>e</sup> )	19.6

<sup>a</sup>Reference 4.

<sup>b</sup>Reference 18.

<sup>c</sup>Reference 3.

<sup>d</sup>Reference 5.

<sup>e</sup>Reference 6.

calculations. Note, however, that the predicted Korringa constants of 124 sec K for  $\text{TiH}_{1.71}$  and 190 sec K for  $\text{TiH}_{1.55}$  yield  $T_{1e}$  contributions which are three times larger than the maximum  $T_1$  values measured on the high-temperature side of the  $T_{1\min}$  and over 50 times larger than the measured  $T_{1\min}$  values.

Hence, even if the predicted Korringa constants are in error by 30%, the calculated  $\tau_d$  errors will be smaller than -27% or +11% for temperatures greater than 500°C and less than 17% for temperatures less than 500°C. While these errors may seem large, they are small compared to differences in predicted values based on the 1NN and 3NN jump models.

For the  $\text{TiH}_{1.71}$  sample, our  $T_1$  measurements between 460 and 520°C were used to calculate  $\tau_d$  in this temperature range. Predicted values of the diffusion coefficient for both jump mechanisms were calculated using Eq. (1), the calculated  $\tau_d$  values, and the known values of  $f_T$  and  $L$ . Figure 3 compares the predicted values to the actual diffusion measurements for  $\text{TiH}_{1.71}$ . Hydrogen motion clearly favors the 1NN jump mechanism and not the 3NN jump mechanism.

The major source of uncertainty in the calculation of the error bars for predicted values of  $D$  in Fig. 3 comes from the value of  $K$  to which we assigned an

uncertainty of 10%.

For the  $\text{TiH}_{1.55}$  sample  $T_1$  measurements between 330 and 560°C were used to calculate  $\tau_d$  values. Predicted diffusion values for 1NN and 3NN jumps are shown in Fig. 7. Note the break in the temperature dependence of the  $D$  values at  $\sim 500^\circ\text{C}$ . It can be seen from Fig. 4 that no such break occurs in the measured diffusion data. The measured  $D$  values show excellent agreement with predictions for 1NN steps up to 500°C and fit nicely with the straight-line extrapolation in Fig. 7 over the remaining 60°C high-temperature interval. This indicates that the breakaway in the  $T_1$  observations above 500°C is unlikely to be connected with a change in the diffusion process. We consider a number of possible explanations for the  $T_1$  behavior: (a) The highest temperature region is characterized by a  $T_{1e}T$  value substantially different from the ( $\sim 190$  sec K) holding for lower temperatures. However, a temperature-dependent Korringa constant that varies substantially over a temperature span of about 500°C (0.04 eV) seems unlikely. (b) A substantial change in hydride concentration results from the high temperatures used for the measurements. However, for the volume of the sample vial used, the pressure-temperature-composition diagram<sup>19</sup> may be used to calculate the increase in partial pressure of hydrogen gas and the corresponding reduction in hydrogen concentration of the titanium hydride. At 650°C, the predicted decrease in hydrogen concentration is less

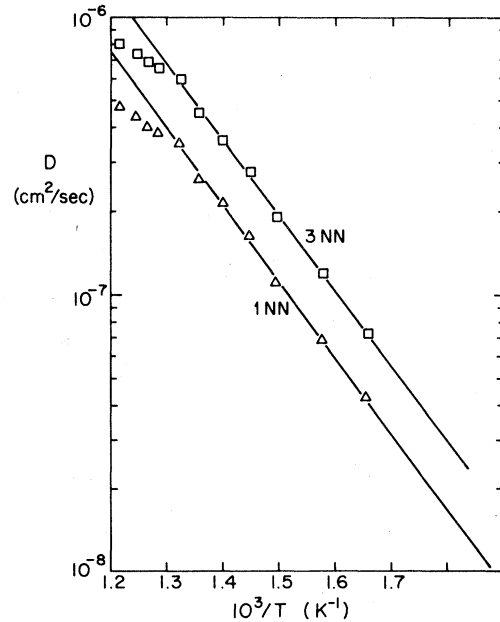


FIG. 7. Predicted values of the diffusion coefficient for  $\text{TiH}_{1.55}$ . The data points are calculated by the first method of Sec. VI. The straight lines are fitted to the data for values of  $(10^3/T) > 1.3 \text{ K}^{-1}$ .

than 0.1%. (c) Since Korn and Zamir measure for  $\beta$ -phase hydrides a  $T_{1e}$ -dominated relaxation rate with Korringa constant  $59 \pm 5$  sec K, the breakaway in  $\tau_d$  evident in Fig. 7 might indicate  $\beta$ -phase behavior. However, the phase diagram of  $\text{TiH}_x$  indicates that if the sample above  $550^\circ\text{C}$  were a mixed phase region, the majority of the hydride would be in the  $\gamma$  phase. For reasonable assumptions regarding the fractional populations of each phase and the exchange rates between phases, the Zimmerman and Britten<sup>20</sup> relaxation theory for multiple phase systems did not satisfactorily explain the  $T_1$  anomaly. In any case, the  $\beta$  phase is characterized by a much larger  $D$  value than the  $\gamma$  phase. Such a transition in diffusion values was not observed by us. (d) Bisson and Wilson<sup>11</sup> predict activation energies of 0.58, 0.69, and 0.65 eV for motion through the octahedral site to first-, second-, and third-nearest-neighbor position. These activation energies are sufficiently close in value that the jump frequency may show a 40% deviation from Arrhenius behavior for the temperature range of 80 to  $550^\circ\text{C}$ . However, this deviation should manifest itself as a gradual curvature and not a sudden shift in slope as evident in Fig. 7. To summarize, we are forced to discard all these suggestions and the anomaly remains unexplained. We conclude that, as in the case of  $\text{TiH}_{1.71}$ , our  $\text{TiH}_{1.55}$  data agree with a model with 1NN steps at least up to  $500^\circ\text{C}$  and most probably beyond.

In the second method, our data were analyzed to simultaneously evaluate  $T_{1d}$  and the Korringa constant using the measured  $T_1$  values for the temperature ranges illustrated in Figs. 5 and 6. As mentioned previously, this required an *a priori* assumption that the jump mechanism for the entire temperature regime is described by a single activation energy, namely

$$\tau_d = \tau_{d0} e^{E_a/kT} \quad (8)$$

Such an assumption was not employed by the analysis illustrated in Figs. 3 and 4. However, this second technique does not require the use of predicted Korringa constants based on Korn and Zamir's results.

Such an analysis was made,<sup>21</sup> using Bustard's Monte Carlo model,<sup>6</sup> for our  $T_1$  data specifically for the 1NN jump mechanism. The results are summarized in Table II. These values of  $E_a$  and  $\tau_{d0}$  are used in the expression

$$D = \left( \frac{f_T L^2}{6\tau_{d0}} \right) \exp(-E_a/kT) \quad (9)$$

to calculate predicted diffusion coefficients to compare with our measured values. Figures 8 and 9 illustrate good agreement between these 1NN hopping model predictions and the measured  $D$  values for both  $\text{TiH}_{1.55}$  and  $\text{TiH}_{1.71}$ .

TABLE II. Activation energies, preexponential factors, and Korringa constants,  $K = T_{1e}T$  obtained by Bustard *et al.* (Ref. 21).

$x = [\text{H}]/[\text{Ti}]$	$E_a$ (eV/atom)	$\tau_{d0}$ ( $10^{-13}$ sec)	$T_{1e}T$ (sec K)
1.55	0.526	0.64	154
1.71	0.543	0.69	91

A similar detailed analysis of the 3NN model was done<sup>22</sup> on an earlier and slightly less accurate version of Bustard's Monte Carlo calculation with the result that the 3NN predictions of  $D$  were about 75% greater than the measured  $D$  values, much like the predicted values in Figs. 3 and 4. Application of the more accurate model<sup>21</sup> would not appreciably alter this disagreement between the 3NN predicted and the measured values of  $D$ .

It will be noted that the Korringa constants in Table II are smaller than those noted in Sec. V. Since these values were deduced using different models relating  $T_1$  to  $\tau_d$  and since the data are over different temperature ranges, the cause of the small discrepancy is not clear. Nevertheless, the conclusion that diffusion favors a 1NN hopping model is clearly

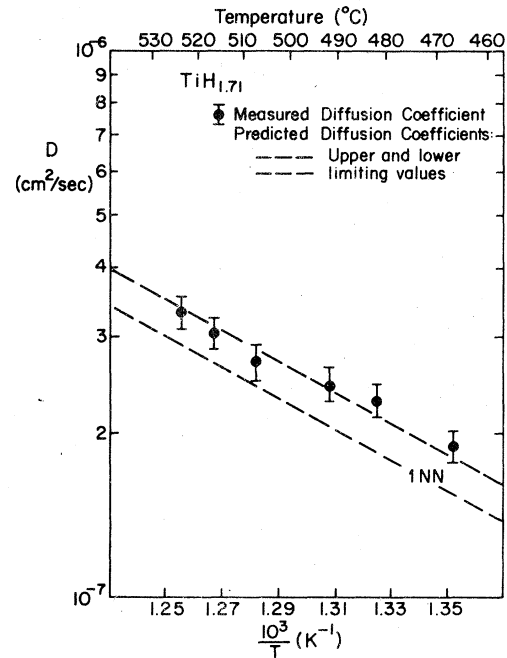


FIG. 8. Measured and predicted values of the diffusion coefficients for  $\text{TiH}_{1.71}$ . Predicted values are based on calculations by the second method discussed in Sec. VI for 1NN hopping.

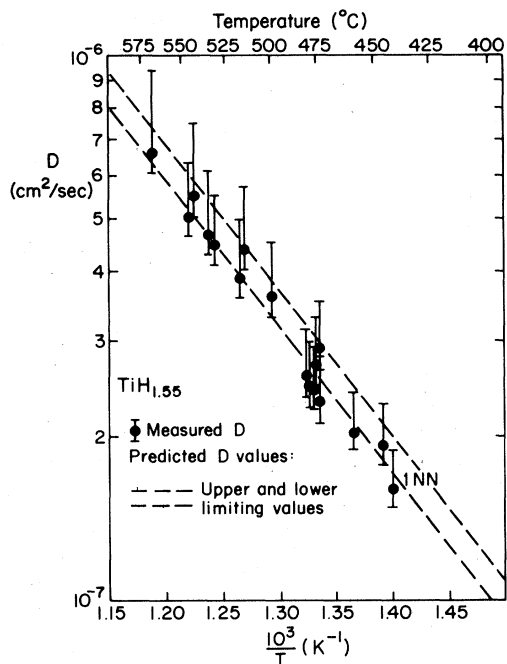


FIG. 9. Measured and predicted values of the diffusion coefficients for  $\text{TiH}_{1.55}$ . Predicted values are based on calculations by the second method discussed in Sec. VI for 1NN hopping.

unaffected by the question of the accuracy of our knowledge of  $K$ .

We do not report on a fitting of our measured values of  $D$  to the Arrhenius relationship. Because of the relatively small range of  $(T)^{-1}$  over which  $D$  was measured, the values  $E_a$  deduced from the data would be less accurate than the values of  $E_a$  of Table II. From our measurements of  $D$ , the values of  $D$  at  $500^\circ\text{C}$  near the middle of the temperature range are

$$D_{1.55} = (3.6 \pm 0.3) \times 10^{-7} \text{ cm}^2/\text{sec}$$

and

$$D_{1.71} = (1.75 \pm 0.1) \times 10^{-7} \text{ cm}^2/\text{sec}$$

By combining these values with values of  $E_a$  from

Table II,

$$D_{1.55} = (9.7 \pm 1) \times 10^{-4} \\ \times \exp(-6.1 \times 10^3/T) \text{ cm}^2/\text{sec}$$

and

$$D_{1.71} = (6.1 \pm 1) \times 10^{-4} \\ \times \exp(-6.3 \times 10^3/T) \text{ cm}^2/\text{sec}$$

where  $T$  is in degrees kelvin. It is interesting to note that the ratio of preexponential factors is 1.59 which is in good agreement with the ratio of vacancy concentrations, 1.55. The existence of a direct proportionality between preexponential factors and vacancy concentrations,  $(2-x)$ , in  $\gamma\text{-TiH}_x$  was proposed by Stalinski, Coogan, and Gutowsky.<sup>23</sup> The uncertainties given for  $D_{1.55}$  and  $D_{1.71}$  are valid over a temperature range from about  $400$  to  $600^\circ\text{C}$ .

## VII. SUMMARY

(i) From measurements of both the diffusion coefficient and the spin-lattice relaxation time it has been shown that hydrogen motion in  $\gamma\text{-TiH}_x$  is predominantly by the first-nearest-neighbor jump mechanism. However, the NMR technique employed cannot distinguish between the two possible jump paths illustrated in Fig. 1. This mechanism, predicted by theoretical calculations by Bisson and Wilson,<sup>11</sup> is confirmed by this experiment.

(ii) A quantitative technique to estimate the size of background gradients has been illustrated, mixing quartz powder with the hydride samples substantially reduced the background gradients and their effects on the measurement of the diffusion coefficient.

## ACKNOWLEDGMENT

Work supported by the National Science Foundation Grants No. DMR73-07521 and No. DMR77-24561.

\*Present address: Sandia Laboratories, Division 4445, Albuquerque, N. M. 87115.

<sup>1</sup>S. S. Sidhu, L. Heaton, and D. D. Zaubers, *Acta Crystallogr.* **9**, 607 (1956).

<sup>2</sup>B. Stalinski, C. K. Coogan, and H. S. Gutowsky, *J. Chem. Phys.* **34**, 1191 (1961).

<sup>3</sup>D. Wolf, *J. Phys. C* **10**, 3545 (1977).

<sup>4</sup>W. A. Barton and C. A. Sholl, *J. Phys. C* **9**, 4315 (1976).

<sup>5</sup>P. A. Fedders and O. F. Sankey, *Phys. Rev. B* **18**, 5938 (1978).

<sup>6</sup>L. D. Bustard, *Phys. Rev. B* **22**, 1 (1980) (preceding paper).

<sup>7</sup>C. K. Coogan and H. S. Gutowsky, *J. Chem. Phys.* **36**, 110 (1962).

<sup>8</sup>C. Korn and D. Zamir, *J. Phys. Chem. Solids* **31**, 489 (1970).

<sup>9</sup>A. Schmolz and F. Noack, *Ber. Bunsenges. Phys. Chem.* **78**, 339 (1974).

<sup>10</sup>H. T. Weaver and J. P. VanDyke, *Phys. Rev. B* **6**, 694 (1972).

<sup>11</sup>C. L. Bisson and W. D. Wilson, in *Effect of Hydrogen on Behavior of Materials*, Proceedings of an International Conference, Moran, Wyoming, 1975, edited by Anthony W.



- Thompson and I. M. Bernstein (American Institute of Mining, Metallurgical and Petroleum Engineers, 1976), p. 416.
- <sup>12</sup>Materials Research Corporation, West Nyack, N.Y.: 10994.
- <sup>13</sup>J. S. Murday and R. M. Cotts, *Z. Naturforsch.* 269, 85 (1971).
- <sup>14</sup>J. E. Tanner, *J. Chem. Phys.* 52, 2523 (1970).
- <sup>15</sup>E. O. Stejskal and J. E. Tanner, *J. Chem. Phys.* 42, 288 (1965).
- <sup>16</sup>H. J. DeBruin and G. E. Murch, *Philos. Mag.* 27, 1475 (1973).
- <sup>17</sup>G. E. Murch (private communication).
- <sup>18</sup>W. A. Barton and C. A. Sholl, *J. Phys. C* 11, 4405 (1978).
- <sup>19</sup>William M. Mueller, James P. Blackledge, and George G. Libowitz, *Metal Hydrides* (Academic, New York, 1968).
- <sup>20</sup>J. R. Zimmerman and W. E. Britten, *J. Phys. Chem.* 61, 1328 (1957).
- <sup>21</sup>L. D. Bustard, R. M. Cotts, and E. F. W. Seymour, *Z. Phys. Chem.* 115, 247 (1979).
- <sup>22</sup>L. D. Bustard, Ph.D. thesis (Cornell University, 1979) (unpublished).
- <sup>23</sup>B. Stalinski, C. K. Coogan, and H. S. Gutowsky, *J. Chem. Phys.* 34, 1191 (1961).